

BELGIAN  
IMPULSE PROGRAMME

**GLOBAL CHANGE**

SYMPOSIUM 17 & 18 MAY 1993  
**PROCEEDINGS**  
VOLUME II

**BELGIAN SCIENCE  
POLICY OFFICE**

## **LEGAL NOTICE**

Neither the Science Policy Office nor any person acting on behalf of the Office is responsible for the use which might be made of the following information.

No responsibility is assumed by the Publisher for any injury and/or damage to persons or property as a matter of products liability, negligence or otherwise, or from any use or operation of any methods, products, instructions or ideas contained in the material herein.

The authors are responsible for the content of their articles.

No part of this publication may be reproduced, stored in a retrieval system, or transmitted in any form or by any means, electronic, mechanical, photocopying, recording, or otherwise, without the prior written permission of the Publisher.

# TABLE OF CONTENTS

## VOLUME I

Section 1 : Atmospheric processes liable to come into play in climate changes

Section 2 : Biogeochemical cycles on land and at sea

## VOLUME II

Section 3 : Global modelling of climate and environment 1

Introduction by Prof. J. JOUZEL 3

Modelling of the climatic system and its response to human activities 5  
Promotor: Prof. A. BERGER

3-Dimensional modelling of the continental cryosphere 31  
Promotor: Prof. H. DECLEIR

Modelling of the vertical processes involved in the global oceanic circulation model  
of Semtner and Chervin 63  
Promotor: Prof. G. PICHOT

Global modelling of the coupled chemical-climatic changes due to human activities  
- part I 91  
Promotor: Prof. J.-C. GÉRARD

Global modelling of the coupled chemical-climatic changes due to human activities  
- part II 121  
Promotor: Prof. G. BRASSEUR

Toward a dynamical view of global change 141  
Promoters: Dr. C. NICOLIS-ROUVAS  
Prof. G. NICOLIS

Section 4 : Past climatic and environmental changes

Introduction by J. JOUZEL 181

Ice composition and global change 183  
Promotor: Prof. R. SOUCHEZ

Climatic short events uncorrelated with the astronomic theory and linked to the reorganization of the oceanic and atmospheric global circulation	201
Promotor: Prof. G. SERET	

**Section 5 : Socio-economic aspects (support to policy making)**

Introduction by C. CASWILL	229
----------------------------	-----

Optimisation of greenhouse gas reduction strategies	
Promoters: Dr. G. WOUTERS	
Prof. S. PROOST	233

Ecophilosophical foundations of a long-term policy concerned with global change	
Promotor: Prof. E. VERMEERSCH	277

**VOLUME III**

**Section 6 : Effects of global change on terrestrial ecosystems, soil, hydrological cycle, ...**

**Section 7 : Support to programme management**

# MODELLING OF THE CLIMATIC SYSTEM AND ITS RESPONSE TO HUMAN ACTIVITIES

by

ANDRE BERGER, JEAN-MICHEL CAMPIN, ERIC DELEERSNIJDER,  
MOHAMED EL MOHAJIR, THIERRY FICHEFET, JEAN-FRANCOIS FOCCROULLE,  
HERVE GRENIER, MIGUEL MORALES MAQUEDA, PHILIPPE TULKENS,  
JEAN-PASCAL VAN YPERSELE

Unité ASTR, Institut d'Astronomie et de Géophysique G. Lemaître,  
Université Catholique de Louvain,  
2 Chemin du Cyclotron, 1348 Louvain-la-Neuve

## Abstract

*Only mathematical models are able to predict the climate change that will be induced over the next decades by the increase of the atmospheric concentration in greenhouse gases. To produce such forecasts it is necessary to work out a model of the Earth's climate system encompassing, at least, the atmosphere, the World Ocean and the sea ice. Such a model is being developed at ASTR.*

*The AGCM of the LMD has been installed at ASTR. This model is briefly described and the first results obtained at ASTR are presented.*

*The sea ice model is of thermodynamic-dynamic type. It is shown that the thermodynamic part, when coupled to a simple ocean model, is giving realistic results. It is believed that an excellent representation of the sea ice cover will be obtained after completing the validation of the thermodynamic part.*

*The free surface OGCM is briefly described. The model has been successfully tested in a robust-diagnostic mode, which means that the main features of the oceanic general circulation are well represented. A first simulation without restoring terms was performed, giving very encouraging results.*

## 1. INTRODUCTION

Since the industrial revolution and, in particular, since a few decades, the human activities have led to a significant increase of the atmospheric concentration in "greenhouse gases". These gases modify the Earth's radiation budget, which could result in a progressive warming of the troposphere during the next decades, *i.e.*, a global climate change that will have an important impact on all activities of Mankind.

The occurrence of the global warming is almost certain (Houghton *et al.*, 1990; Houghton *et al.*, 1992), but the detailed knowledge of the climate change is not yet available. However, accurately predicting the way the climate will modify is necessary for the Society to make decisions that will minimize the costs of the global warming. It is thus important that the methods for predicting the future climate of the Earth's be improved.

Only mathematical models can take up the challenge of accurately forecasting the evolution of Earth's climate system.

The Earth's climate system consists in the atmosphere, the biosphere, the cryosphere, the lithosphere and the World Ocean. All those parts do not evolve separately: they are exchanging matter, momentum and energy. As a consequence, a realistic climate model must encompass all the components of the climate system. Nevertheless, building a reliable model of the whole system is an enormous task. Furthermore, it is widely believed that predicting, with an acceptable degree of realism, the evolution of the climate on time scales of a few decades can be achieved by implementing a coupled atmosphere-ocean-sea ice model.

The roles of these three components of the climate system may be summarized as follows. The atmosphere and the ocean transfer heat from the Equator to the Poles, the poleward fluxes in the two sub-systems being of the order of a few  $10^{15}$  Watts (Cariù *et al.*, 1985; Peixoto and Oort, 1992). The sea ice formation and melting involves significant amount of heat, which may not be neglected. Furthermore, the seasonal sea ice cycle greatly modifies the thermohaline structure of the water masses, which has an important impact on the general circulation. Finally, there are numerous important interactions and feedback mechanisms between the atmosphere, the World Ocean and the sea ice.

The Institut d'Astronomie et de Géophysique G. Lemaître (Unité ASTR) of the Université Catholique de Louvain has decided to set up such a three component model of the climate system. To do so, we are developing an Oceanic General Circulation Model (OGCM) and a sea ice model. We are using the Atmospheric General Circulation Model (AGCM) of the Laboratoire de Météorologie Dynamique (LMD) of the C.N.R.S. (Paris). We also have many collaborative projects with other research institutions in Belgium and in France.

In the present paper we report on the development, the implementation and the validation of the above-mentioned models. Preliminary results are also presented and discussed.

## 2. THE AGCM OF THE LMD

The AGCM provided by the LMD is definitely the most complex of the models operated at ASTR in the scope of the Global Change programme. Plenty of publications — referred to in Grenier (1993) — have been devoted to all aspects of this model and to its comparison with other AGCMs. Here, it suffices to say that LMD's model is widely acknowledged as one of the

state-of-the-art models capable of being used for climate studies (Cess *et al.*, 1990). Details about the implementation of LMD's AGCM at ASTR may be found in Grenier (1993).

Before presenting some results obtained at ASTR, it is necessary to briefly describe LMD's AGCM.

## 2.1. The LMD model and its implementation at ASTR

LMD's AGCM is a primitive equations model, which rests on classical hypotheses: the hydrostatic equilibrium is assumed to be valid, the equation of state of the air is that of a perfect gas and the height of the atmosphere is considered negligible compared with the Earth's radius. The vertical coordinate is the so-called sigma coordinate, *i.e.*, the ratio of the pressure to the pressure at ground level (Phillips, 1957). Using this coordinate system has the noticeable advantage that the limits of the computational domain are coordinate surfaces.

The main dependent variables are the horizontal velocity components, the transformed vertical velocity associated with the sigma coordinate, the geopotential, the surface pressure, the potential temperature, the water vapor concentration and the liquid water concentration.

Numerous parameterizations are involved in the model. Particular attention has been devoted to the definition of a cloud fraction. This original scheme is described in Le Treut and Li (1991). The radiative code is an improved version of the parameterizations originally devised by Fouquart and Bonnel (1980) for the short waves and Morcrette (1991) for the long waves. Three convective adjustments algorithms are called on, *i.e.*, dry adjustment, wet adjustment and Kuo-type adjustment. The first two aim at the representation of atmospheric convection when the air column is unstable, while the last is called on to take into account the large-scale cumulus convection process, mainly in tropical regions. The roughness length is different from point to point, according to the nature of the soil and its vegetation. In the most recent version, a soil model (Ducoudré *et al.*, 1993) is invoked in order to properly represent the water exchanges between the ground and the atmosphere, which permits studying the effects of deforestation (Polcher and Laval, 1993). The vertical eddy diffusivities are obtained from a turbulence closure which might well be too crude, since it rests on simple equilibrium assumptions. Improving this aspect of the model is presently being considered by the LMD.

To obtain the numerical solution to the equations of the model, the finite difference technique is used — which is not always the case in AGCMs, since many of them rely on spectral decomposition of the unknowns in the horizontal plane. The numerical grid covers the whole Earth. In the commonly used version of the program, there are 64 equally spaced grid points in the longitudinal direction, meaning that the longitudinal resolution is  $360^\circ/64 \approx 5.6^\circ$ . Fifty grid points are distributed according to the sine of the latitude between the North Pole and the South Pole, which implies that there is only one grid point between the latitude  $\pm 78.5^\circ$  and  $\pm 90^\circ$ . In other words, model's resolution is rather coarse in the polar regions, which will probably require some adaptations when we will proceed towards the coupling with the sea-ice model and the OGCM. There are 11 levels in the vertical direction. The latter are distributed in such a

way that approximately 4 levels are located in the planetary boundary layer, while about 3 of them are in the stratosphere — the last grid point being at a height of about 30 km above the sea level.

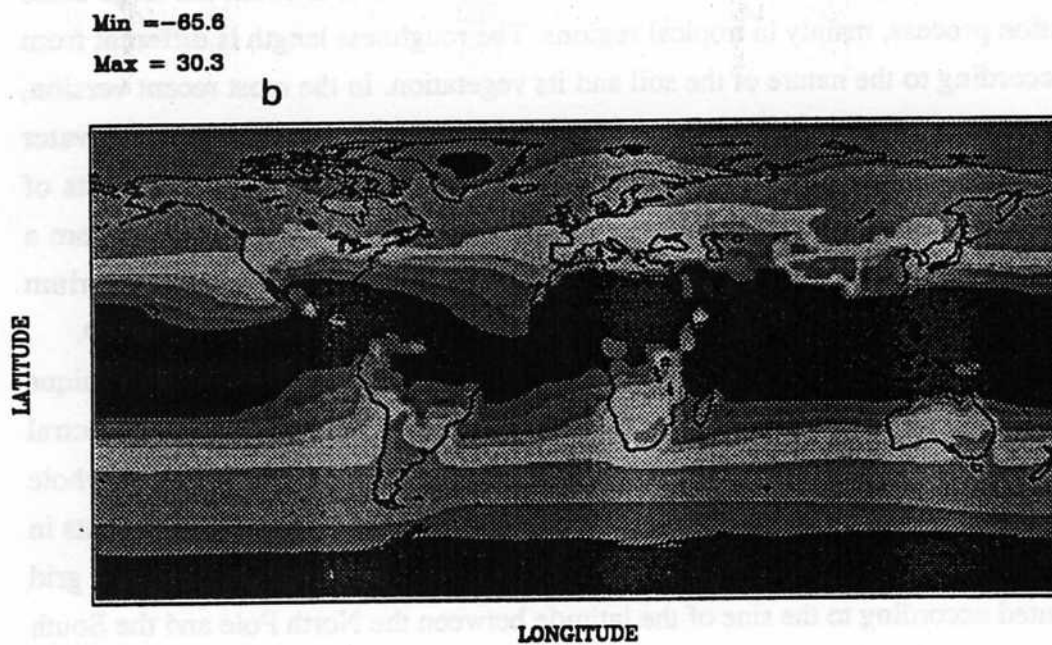
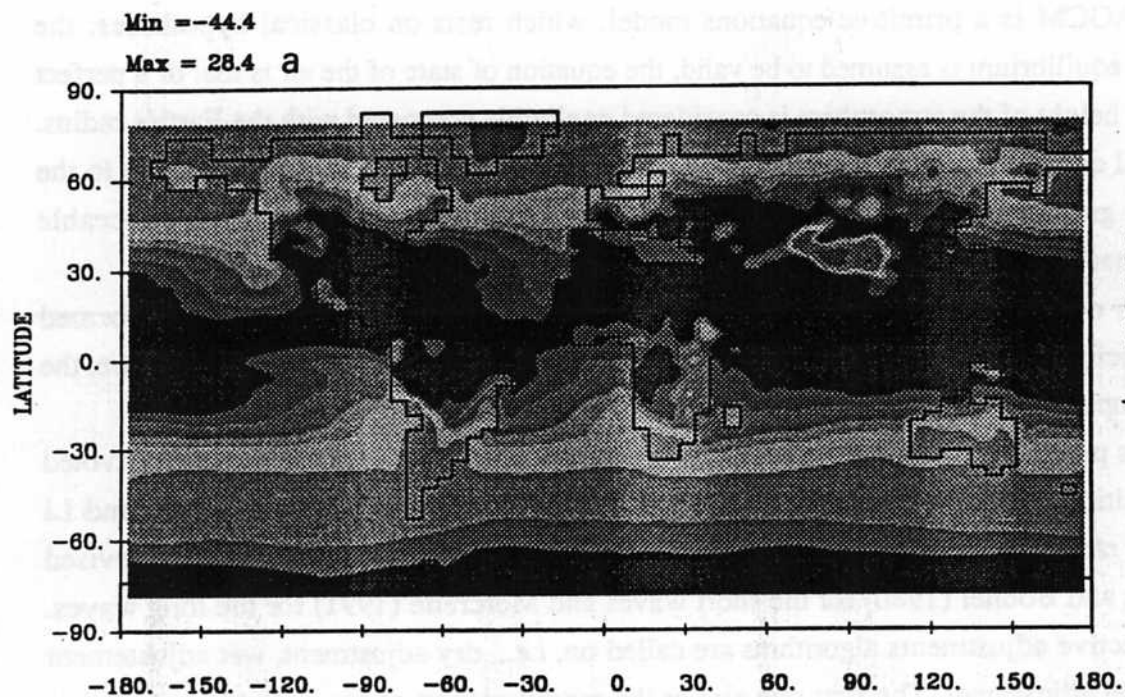


Figure 2.1. Surface temperature in July-August predicted by the AGCM (a) compared with the NCAR climatology (b).



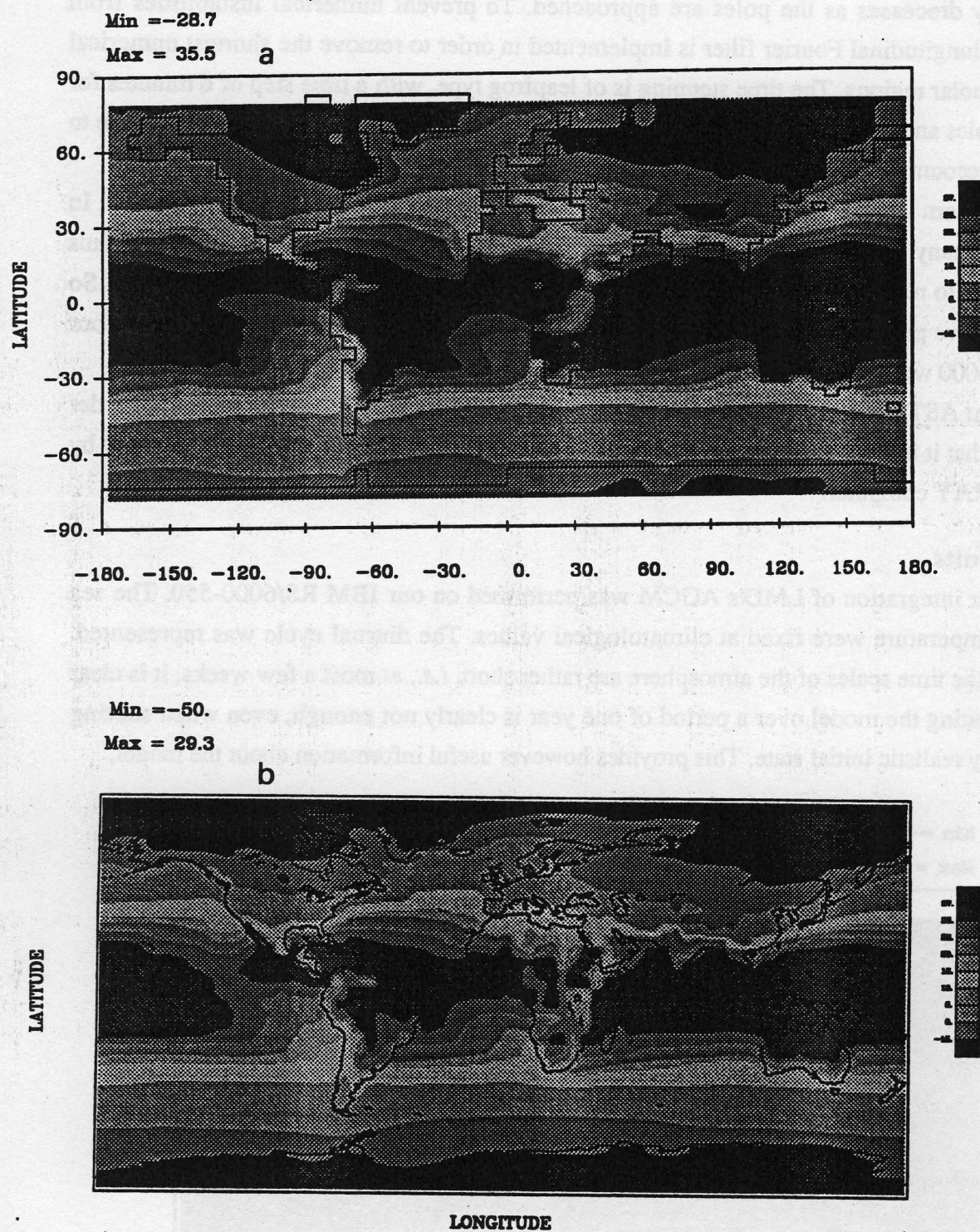


Figure 2.2. Surface temperature in January predicted by the AGCM (a) compared with the NCAR climatology (b).

Because of the equal longitudinal spacing of the grid points, the west-east mesh size drastically decreases as the poles are approached. To prevent numerical instabilities from arising, a longitudinal Fourier filter is implemented in order to remove the shortest numerical waves in polar regions. The time stepping is of leapfrog type, with a time step of 6 minutes for the dynamics and 30 minutes for the "physics". With such a time stepping, the model is able to take into account the diurnal cycle.

The program is written in FORTRAN 77 and has been optimized for CRAY computers. In particular, many specific CRAY instructions rendered the program non-portable. We have thus been forced to remove those special instructions and to modify the program appropriately. So doing we have produced a portable version of the LMD model, which we have installed on our IBM RS/6000 workstation. This work will be detailed in a forthcoming progress report.

So far, at ASTR, we have thoroughly tested the portable version of LMD's AGCM in order to ensure that it is "bug-free" and that it produces the same results as those obtained at LMD by using a CRAY computer.

## 2.2. Results

A one year integration of LMD's AGCM was performed on our IBM RS/6000-550. The sea surface temperature were fixed at climatological values. The diurnal cycle was represented. Although the time scales of the atmosphere are rather short, *i.e.*, at most a few weeks, it is clear that integrating the model over a period of one year is clearly not enough, even when starting from a very realistic initial state. This provides however useful information about the model.

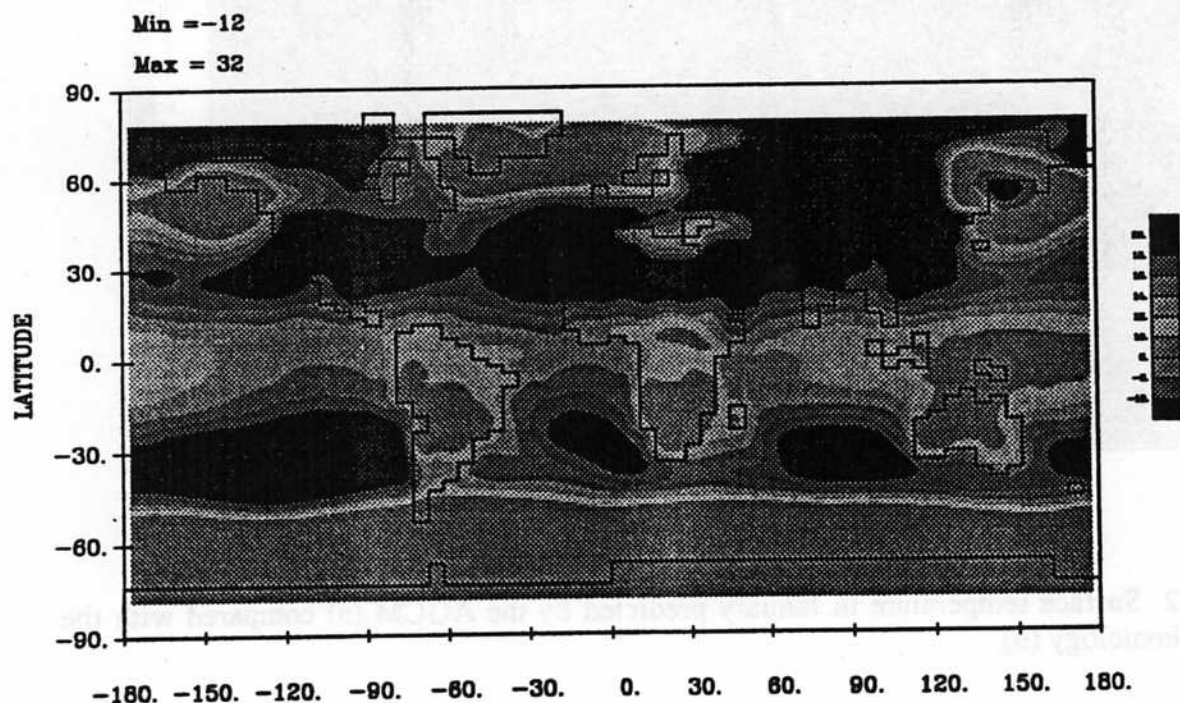


Figure 2.3. Sea level pressure - 1000 in december (in Hecto-Pascal).

The Figures 2.1 and 2.2 represent the surface temperature computed by the model and the observed values (from the NCAR climatology) for summer and winter months. In general, there is a good agreement between the predictions of the model and the observations. It must be pointed out that the seasonal cycle is properly represented. Nevertheless, the continents are too warm in the summer hemisphere and too cool in the winter hemisphere. This is partly due to the poor representation of the land-atmosphere interactions in this version of the model. A improved version is being installed (Polcher and Laval, 1992; Ducoudré *et al.*, 1993).

The sea level pressure also gives useful indications about the behaviour of the model (Figure 2.3). The main features of the geographical distribution of the sea level pressure are properly simulated, namely the low pressures in the high latitudes of the Southern Hemisphere, the high pressures over the continents in the winter hemisphere and over the oceans in the summer hemisphere. For instance, the Iceland Low is correct, while the Aleutian Low is somewhat too deep. Longer simulations would allow to determine more correct long term means, as was done by Cubash *et al.* (1992), for example.

### 3. THE SEA-ICE MODEL

The thermodynamic processes involved in the buildup of sea-ice in interaction with the upper ocean are relatively well understood and modelled (*e.g.* Semtner, 1976; Fichefet and Gaspar, 1988; Björk, 1988). Present efforts are mainly directed towards comprehensive thermodynamic-dynamic models in which ice motion and ice-ice interactions are taken into account. Dynamics dominates ice ridging and formation of open water regions within the pack leading to major feedbacks between thermodynamic processes and transport. Ice motion and deformation are computed as functions of the atmospheric/oceanic forcings and the state of ice (*e.g.* Hibler, 1980; Flato and Hibler, 1992).

ASTR is developing a thermodynamic-dynamic sea-ice model capable of being coupled with an AGCM and an OGCM. This model includes a representation of leads and a bulk rheology. Ice thermodynamics and ice dynamics are coupled through advection processes. At the present time, for testing purposes, the sea-ice model is coupled to a simple oceanic mixed layer and pycnocline model, which is derived from Gaspar (1988) and is presented in Fichefet and Maqueda (1993). The atmospheric forcings are provided by the results of the EMERAUDE AGCM of Météo-France (Toulouse). In the present report, some details are given about the sea-ice model only.

#### 3.1. Sea-ice thermodynamics

The formulation of the thermodynamic part of the sea-ice model is essentially that of Fichefet and Gaspar (1988). According to Semtner (1976), a three-layer snow-ice sheet is considered. The temperature profile within the snow is linear between the air-snow and the snow-ice

interfaces. The two layers of ice have equal thicknesses and their temperatures are computed from a one-dimensional heat-diffusion equation. A heat reservoir stores the shortwave radiation absorbed within the ice during the summer, parameterizing in this way the presence of brine pockets within the ice that, by melting and freezing, slow down any heating of the ice sheet during spring or any cooling during fall.

The heat flux between the ocean and the ice,  $F_b$ , is computed by assuming that sea-ice is in thermodynamic equilibrium with the underlying water, implying that the mixed-layer temperature is that of the freezing point,  $T_f$ . Thus, at the ice-water interface, the heat budget reads

$$F_b = F_{ent} + F_{dif} + F_{tra} + F_{fus}, \quad (3.1)$$

where  $F_{ent}$  and  $F_{dif}$  are the entrainment and diffusion heat fluxes at the base of the pycnocline,  $F_{tra}$  is the solar irradiance transmitted through the ice and absorbed in the mixed layer and  $F_{fus}$  is the heat flux released or absorbed by the mixed layer in order to follow the changes of  $T_f$  due to changes in salinity.

One of the key points of the thermodynamic model is the parameterization of leads, or lanes, *i.e.*, regions of open water scattered within the region occupied by pack ice. The presence of leads allow the direct transmission of heat, momentum, and mass between the ocean and the atmosphere in regions otherwise covered by ice. In particular, the sensible heat flux through the leads seems to play a major role in keeping a relatively warm surface air temperature in winter. To account for these processes, a fraction of the surface of each grid box is assumed to be ice-free and is computed from the energy budget of the leads (Fichefet and Maqueda, 1993). The lead fraction is assumed to be at any time greater or equal than a lower limit, because cracks or leads are always present in the ice cover.

### 3.2. Sea-ice dynamics

Parameterizing the ice motion, even in a simple manner, is of high importance for the model to be able to properly reproduce the sea-ice distribution and thickness. Indeed, the transport of ice towards warmer latitudes places a limit to the ice extent in winter and prevents the accumulation of ice in near shore regions.

It may be shown that inertia forces acting on the sea-ice sheet are negligible for time scales longer than about half an hour (Rothrock, 1973; Thorndike, 1986). Keeping in mind this simplification, the momentum equation may be written as

$$\tau_{ai} + \tau_{wi} - mg\nabla\eta - mfe_z u + F_{rh} = 0, \quad (3.2)$$

where  $g$ ,  $\eta$ ,  $f$ ,  $\nabla$ , and  $e_z$  are the gravitational acceleration, the sea surface elevation, the Coriolis factor, the horizontal "gradient" operator, and the vertical unit vector, respectively;  $m$  and  $u$

denote the ice mass per unit area and the ice velocity vector;  $\tau_{ai}$ ,  $\tau_{wi}$ , and  $F_{rh}$  represent the stress at the air-ice interface, the water-ice stress, and the stress due to ice-ice interactions. Classical quadratic parameterizations of the interfacial stresses are used (McPhee, 1975; Brown, 1979). The internal forces  $F_{rh}$  are expressed according to Semtner's (1987) simplification of Hibler's (1979) visco-plastic rheology (Fichefet and Maqueda, 1993).

As mentioned earlier, the advective processes link the thermodynamic and the dynamic parts of our sea-ice model. Owing to the importance of this coupling, it was decided to implement an advection scheme of high quality. Prather's (1986) algorithm was selected, because of its capacity of enforcing positivity constraints and conserving moments up to the second order. The advected quantities are the ice compactness — or ice concentration —, the mean snow and ice thicknesses, as well as the thermal contents of the two ice layers.

### 3.3. Results

The model is global and is written in spherical coordinates. The grid, which is of B type, encompasses 128 points in the longitudinal direction and 64 points in latitude.

The atmospheric and oceanic forcings are described in Fichefet and Maqueda (1993). At the present time, the dynamic part of the model is being tuned so that no results involving this part of the code is presented. A 20-year run has been performed in order to reach an equilibrium state — as regards the ice extent.

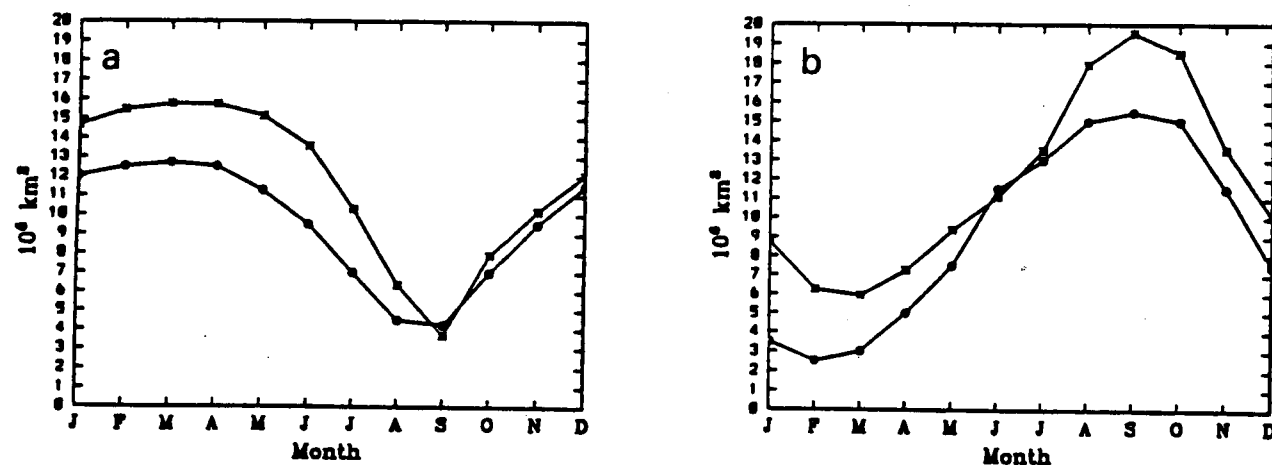


Figure 3.1. Monthly mean sea-ice area (in  $10^6 \text{ km}^2$ ) in the Northern Hemisphere (a) and the Southern Hemisphere (b). The symbol "o" corresponds to the observations of Parkinson *et al.* (1987) for the Northern Hemisphere and Zwally *et al.* (1983) for the Southern Hemisphere, while "\*" indicates model results.

Figure 3.1.a compares the seasonal cycle of the Northern Hemisphere sea-ice area calculated by the model with the satellite observations of Parkinson *et al.* (1987). During fall, the modelled ice extent is in general agreement with the data, whereas the quality of the prediction



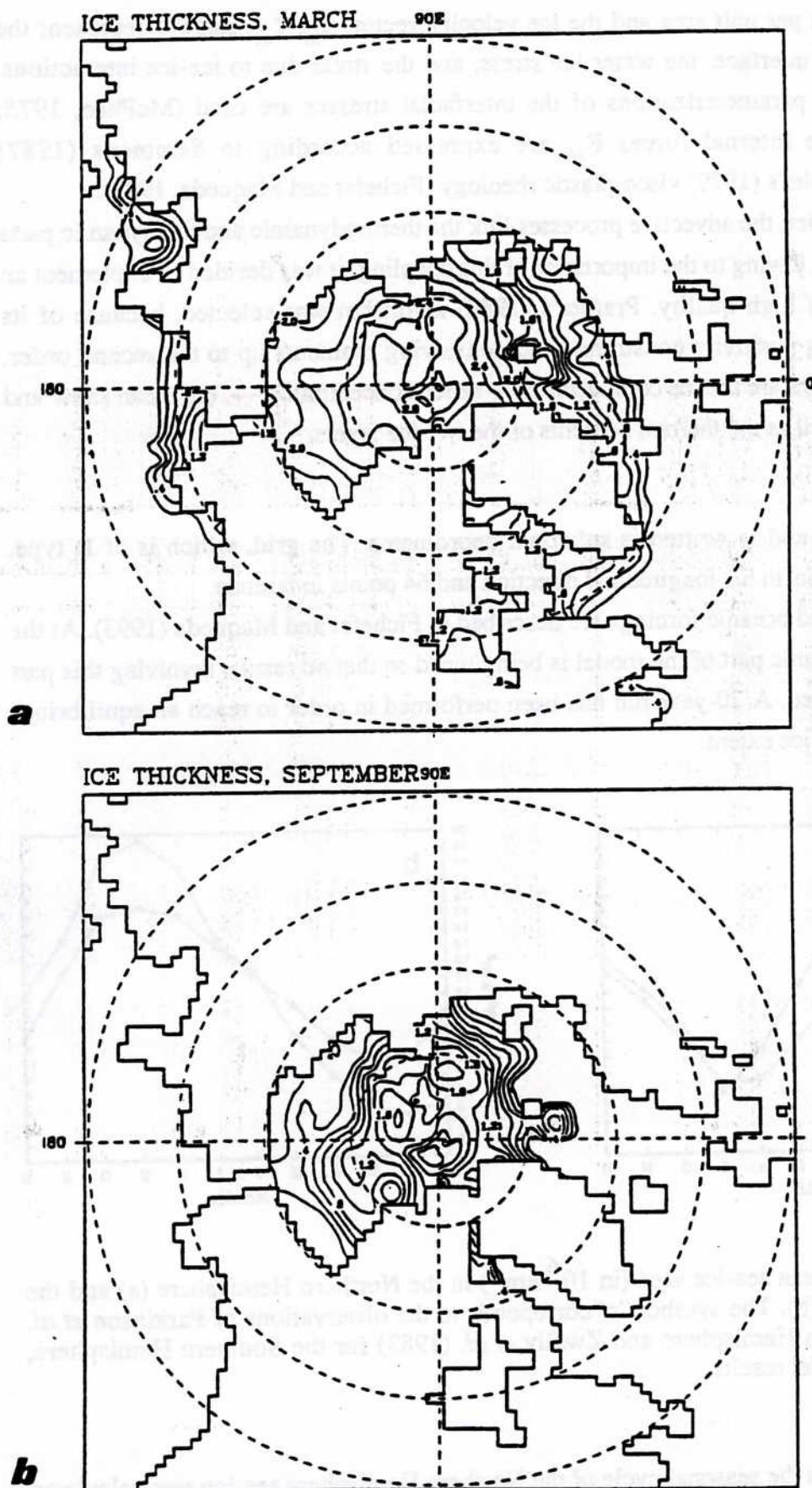
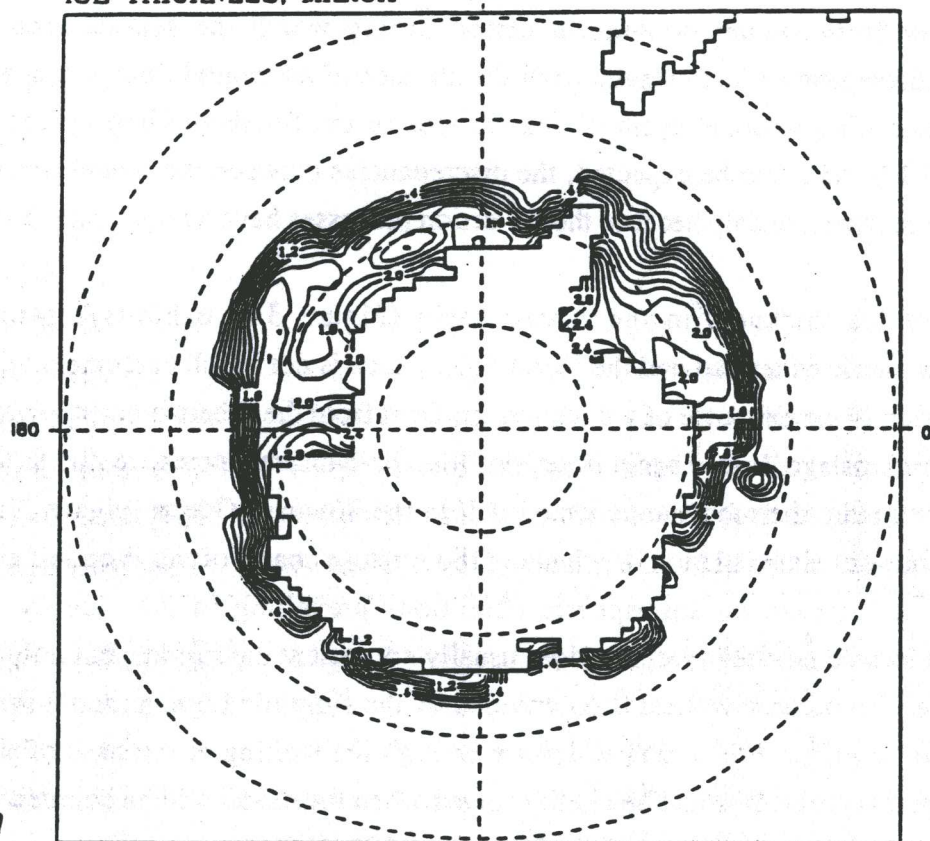


Figure 3.2. Simulated ice thickness (in meters) for the Northern Hemisphere in March (a) and September (b).

ICE THICKNESS, MARCH

90W



ICE THICKNESS, SEPTEMBER

90W

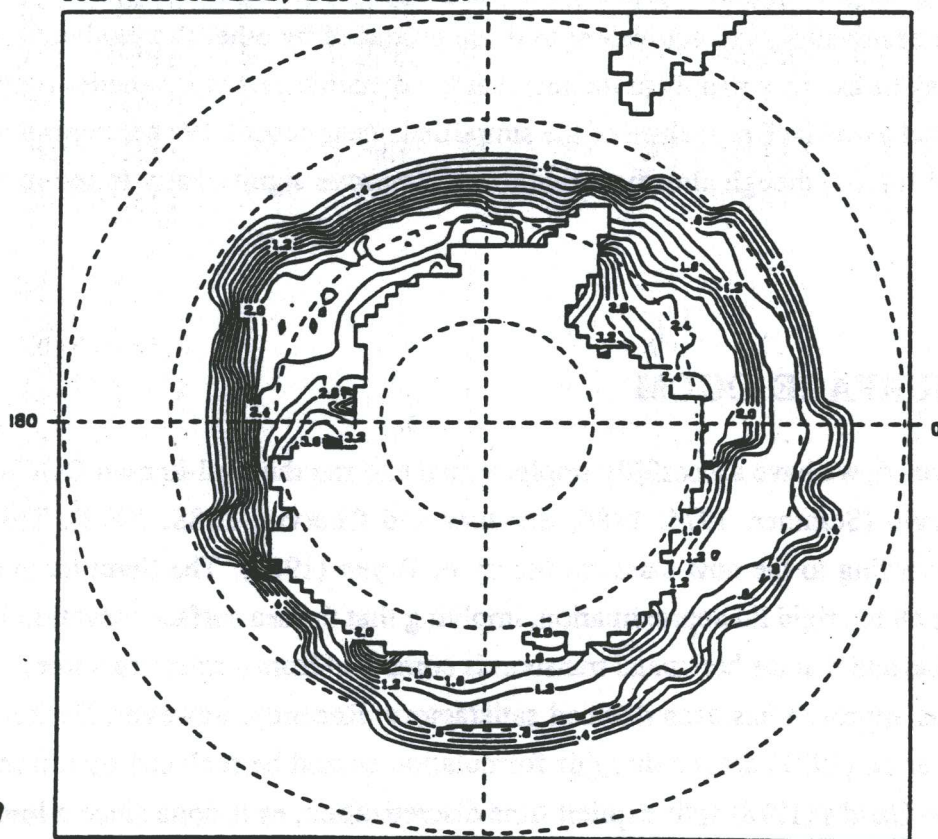


Figure 3.3. Simulated ice thickness (in meters) for the Southern Hemisphere in March (a) and September (b).

is significantly lower from January to June, a period during which the sea-ice area is overestimated. This discrepancy mainly results from the absence of horizontal transport in the model ocean used here. The seasonal cycle of sea-ice area in the Southern Hemisphere is displayed in Figure 3.1.b. As could be expected, the discrepancies between the model results and the observations are larger, mainly because the advection processes have a major role in the Southern Ocean.

The distribution of ice thickness in the Arctic basin (Figure 3.2) exhibits a rather homogeneous and symmetric pattern around the North Pole, which is not in full agreement with the observations pointing to the existence of a thickness gradient from the Siberian coast toward the North Canadian Archipelago. It may again be argued that these discrepancies are due to the limitations inherent in a mere thermodynamic ice model. In the Southern Ocean (Figure 3.3), the model produces spurious accumulation of ice along the western coasts of the Weddell and Ross Seas. Because of the extreme atmospheric conditions prevailing in the vicinity of Antarctica, the sea ice located near the continent does usually not melt at the surface, but only at the ice-water interface. The oceanic vertical flux provided by the simplified ocean model used here does not seem to be sufficiently strong to ensure enough ice melting at the base of the pack. It is believed that this problem would be readily solved when the model will be coupled to a realistic OGCM, as indicated in the results of van Ypersele (1986, 1990).

Overall, the results presented here are extremely encouraging. The discrepancies between the model results and the observations are equivalent to those produced by other thermodynamic sea-ice models and may be ascribed mainly to the fact that the dynamic part of the model is not yet fully operational and to the lack of realism of the simplified ocean model. We are confident that the sea-ice model results, though already realistic, will improve significantly in the near future.

## 4. THE FREE-SURFACE OGCM

As was originally planned, we have successfully implemented and ran the well-known OGCM of Semtner and Chervin (Semtner, 1974, 1986; Semtner and Chervin, 1988, 1992). This model is designed according to the now classical theory of Bryan (1969). The Semtner and Chervin OGCM relies on the rigid lid approximation, implying that the sea surface elevation is not a prognostic variable and that the horizontal transport is computed from a streamfunction.

For many years, this approach has been deemed satisfactory. Recently, however, Beckers (1991) and Killworth *et al.* (1991) argued that this formulation should be replaced by a free-surface one, relying on Gadd's (1978) split-explicit time discretization, as is done since a long time in shallow sea models (Blumberg and Mellor, 1987) and in atmospheric models (Gadd, 1978). The reasons put forward by Killworth *et al.* (1991) were as follows.



First, “the necessity to make several hundred relaxations of a streamfunction per time step might need about as computation as would the taking of several hundred small surface gravity-wave-limited time steps for the barotropic component of a free-surface model” (Killworth *et al.*, 1991).

Second, it must be realized that satellite altimetric data are going to be more and more numerous and accessible (Koblinsky *et al.*, 1992). Moreover, the sea surface elevation is one of the very few variables that will be routinely measured at a truly global scale with a rather high sampling frequency. Thus, having the sea surface as a prognostic variable will certainly facilitate the use of altimetry information, for the purposes of calibration, validation or data assimilation.

Finally, the tides, which probably play a crucial role in the exchanges of matter, momentum and energy between the oceans and the shelf seas, cannot be accounted for if the surface gravity waves are not present in the model.

We found this reasoning rather convincing and we decided to embark in the working out of a free-surface OGCM. Instead of abandoning the Semtner and Chervin code, we decided to use it as a unique tool to help us design, calibrate and validate our own model.

The development of our OGCM is not yet completed. However we have already obtained numerous encouraging results. We are thus inclined to think that our initiative will be crowned with success.

#### 4.1 Equations and numerics of ASTR's OGCM

ASTR's OGCM is a primitive equation model resting on the usual set of assumptions, *i.e.*, the hydrostatic equilibrium and the Boussinesq approximation. The main dependent variables are the sea surface elevation, the three components of the velocity, the potential temperature and the salinity.

The vertical turbulent fluxes are parameterized with the help of eddy diffusivities. For the moment, the latter are computed according to the simple formulae of Pacanowski and Philander (1981). However, in the near future we will implement a more sophisticated turbulence closure. The choice of the turbulence closure to be implemented has not yet been made. In collaboration with MUMM (Brussels) we are examining and testing some well known turbulence closures in the perspective of their introduction in an OGCM (Maqueda and Fichefet, 1991; Van den Eynde, 1992; Deleersnijder and Luyten, 1993).

The space discretization is based on the “finite volume” technique on the B grid. In the horizontal plane, spherical coordinates are used, while the so-called “z-coordinate” is underlying the vertical discretization.

The time discretization is based on an Euler forward time stepping, by contrast with most OGCMs where a leapfrog method is used. We believe that this choice leads to a somewhat simpler numerical scheme and that it does not involve significant drawbacks. On the contrary, the way the computations are organized naturally leads to a forward-backward time stepping for

both the external and internal gravity waves, which is more accurate than a leapfrog one (Mesinger and Arakawa, 1976). Furthermore, most of the accurate discretizations of the advection terms available in the literature rest on a forward discretization of the time derivatives. As regards the advection terms, we have selected a “TVD-like” scheme (James, 1986) extended to three space dimensions through a fractional step approach. This is detailed in Deleersnijder and Campin (1993a). It must also be pointed that the vertical fluxes are computed implicitly, which will allow us to use fine vertical resolution — required by a turbulence closure model — while keeping sufficiently high values of the time step without risking numerical instability.

In order to speed up the calculations, it is possible to use a convergence accelerator (Bryan, 1984). To avoid the severe limitation on the time step set by the external gravity waves, we have recourse to the split-explicit technique (Gadd, 1978; Madala, 1981; Killworth *et al.*, 1991), which consists in calculating the external mode and the internal mode separately. The equations of the external mode are the depth-integral of the horizontal momentum equations and the depth-integral of the continuity equation,

$$\frac{\partial \eta}{\partial t} + \nabla \cdot \mathbf{U} = 0, \quad (4.1)$$

where  $\mathbf{U}$  is the horizontal transport. Although the external mode is advanced in time with a short time step, the external mode calculations require about 10% of the total CPU time only, for the external mode equations are two-dimensional. The internal mode equations are three-dimensional and are concerned with a much longer time step.

Presently the model runs on a coarse  $5^\circ$  by  $5^\circ$  degree spherical grid, closed at  $65^\circ$  N, with 9 levels in the vertical direction, the spacing of which is given in the figures below. The external mode time step is 10 minutes. The internal mode time step for the dynamics is equal to 2 hours, while that for the temperature and salinity equations is 24 hours.

In the near future, the model will be implemented on a  $2^\circ$  by  $2^\circ$  grid covering the North Pole. This will be done by patching two spherical grids. The first one is a standard spherical grid covering the whole World Ocean, except the Northern Atlantic and the Arctic, which are represented in a spherical coordinate grid having its poles on the equator. The linking of the two grids is made in the equatorial Atlantic without any problems, because the coordinate lines of the two grids coincide on the Equator. With such a practice, there is no need to resort to a Fourier filter at high latitudes or to use a more complex technique involving a sophisticated curvilinear coordinate system to avoid the North Pole singularity.

In the numerical experiments presented here, the model is forced with the annual mean of the wind stress (Hellerman and Rosenstein, 1983) and the temperature/salinity data of Levitus (1982) are used. The surface temperature and salinity are forced to remain close to the observed values by means of a restoring term involving a time scale of one week. The same kind of restoring term is utilized in the meshes adjacent to the artificial impermeable wall at  $65^\circ$  N in the

Atlantic. In this region, we found it appropriate to introduce a restoring time scale of one month.

#### 4.2 The robust-diagnostic experiment

We first performed robust-diagnostic experiments, which allows to reach a steady state within a few years. In those run, the temperature and salinity computed by the model are forced towards the observations with the help of a restoring term having a time scale of 2 years. In this mode, the thermohaline structure of the model is thus not completely free, implying that this kind of experiment mainly constitutes a test of the dynamical part of the model.

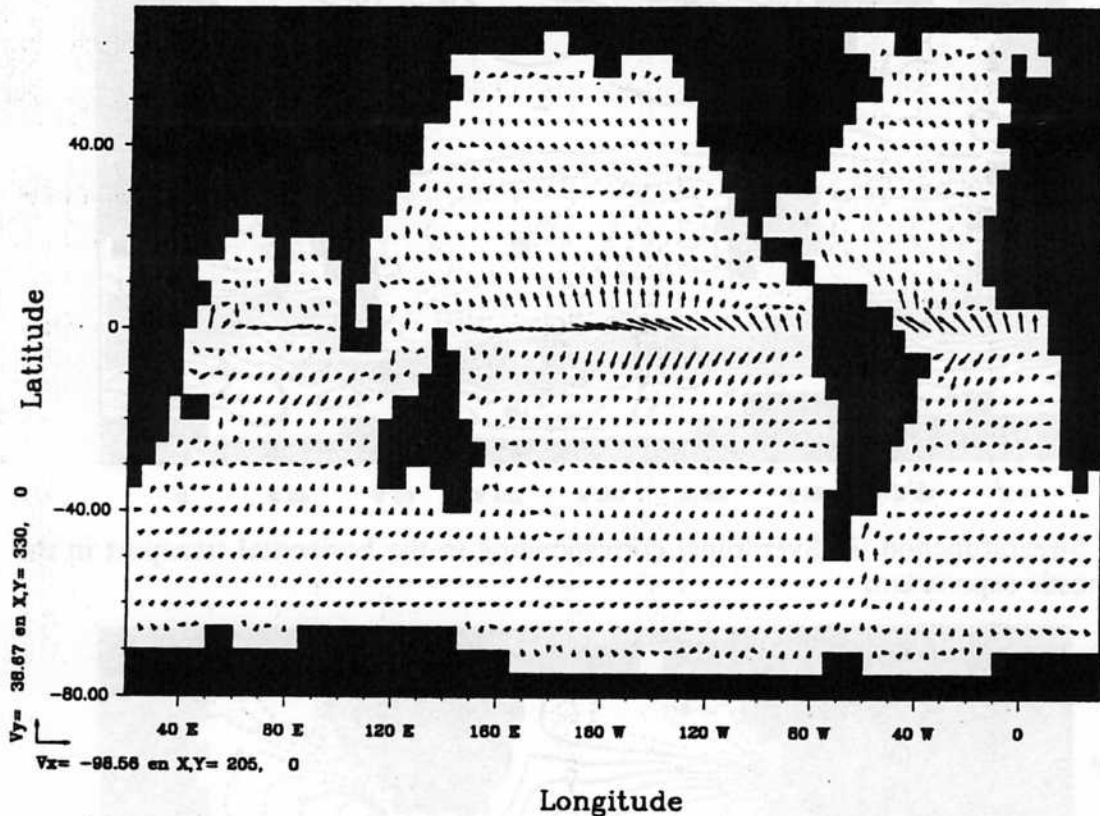


Figure 4.1. Surface currents predicted in the robust diagnostic mode.

The steady state results clearly show that the model is able to reproduce the main features of the general circulation in the World Ocean (Figure 4.1 and 4.2). For example, the flow through Drake passage is about 110 Sverdrups, the circulation in the Northern Atlantic gyre is approximately 20 Sverdrups and that of the Northern Pacific gyre is roughly speaking 40 Sverdrups.

The sea surface elevation seems to be in rather good agreement with the first data of the TOPEX/POSEIDON satellite (Gaspar, 1993, personal communication) (Figure 4.3).

The meridional overturning circulation (Figure 4.4 and 4.5) is comparable to that obtained with models having a similar resolution or even a finer (Semtner and Chervin, 1988;

Toggweiler *et al.*, 1989; Maier-Reimer *et al.*, 1991; Marti, 1992; Semtner and Chervin, 1992). In the Antarctic region the meridional circulation is about correct, whereas the overturning circulation is probably a bit weak in the Northern Atlantic, which may certainly be ascribed to the fact that the region of deep water formation is outside the present computational domain.

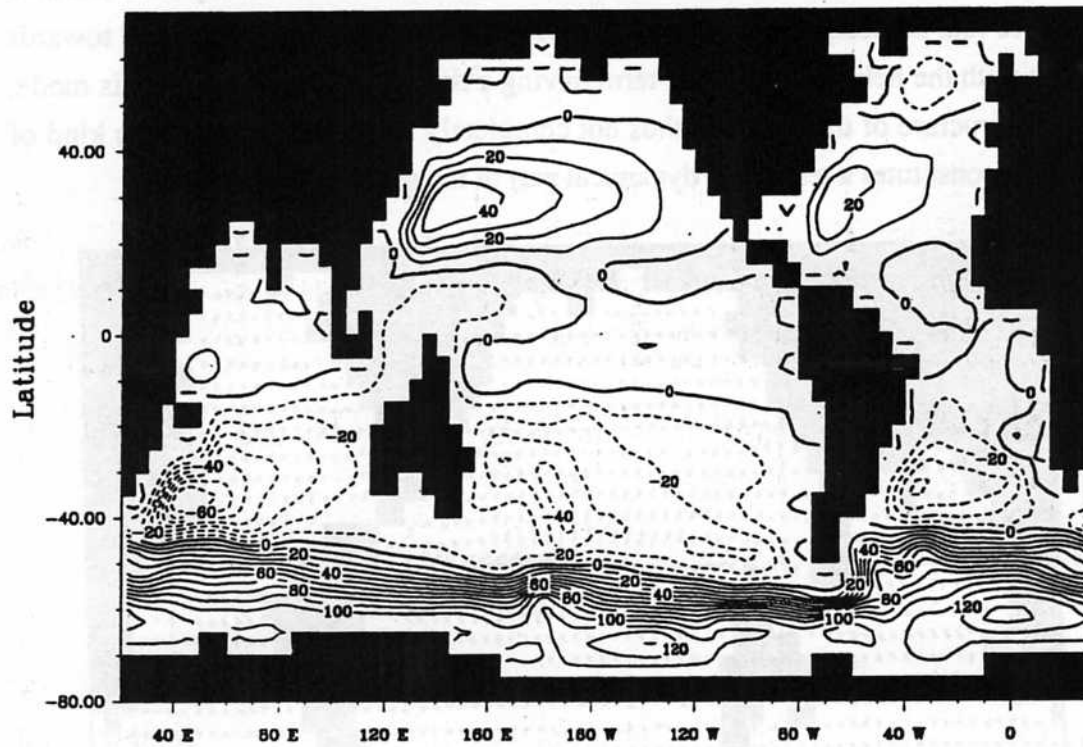


Figure 4.2. Streamfunction (in Sverdrups) corresponding to the horizontal transport in the robust diagnostic experiment.

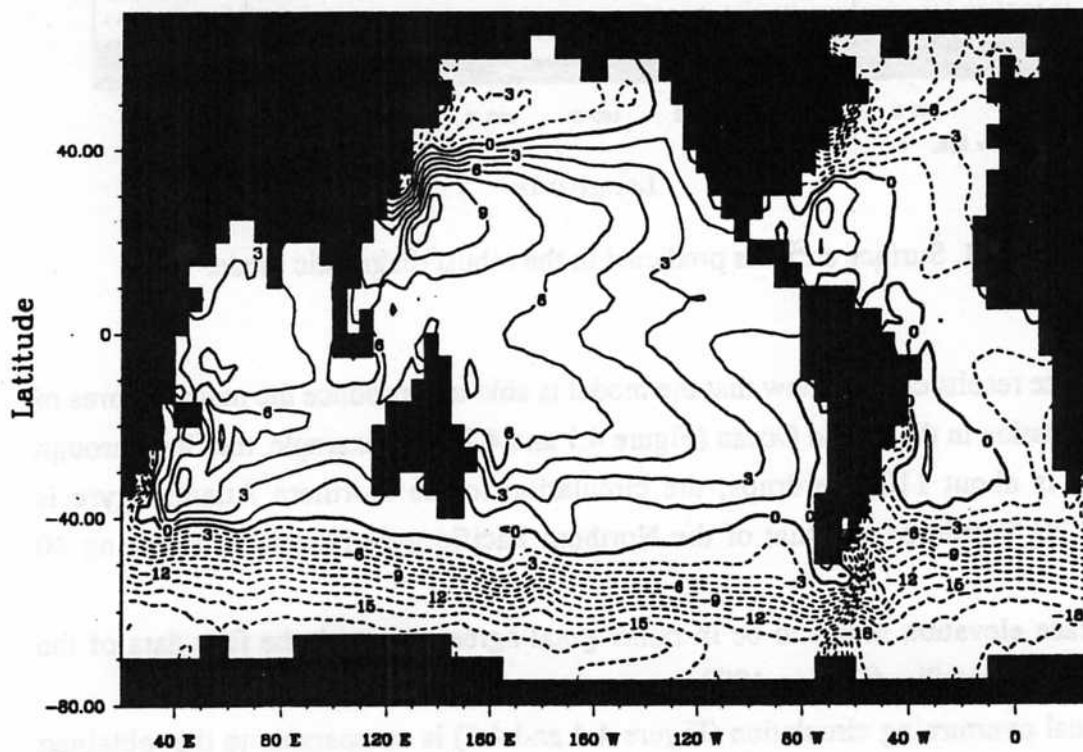


Figure 4.3. Sea surface elevation (in decimeters) in the robust diagnostic experiment.

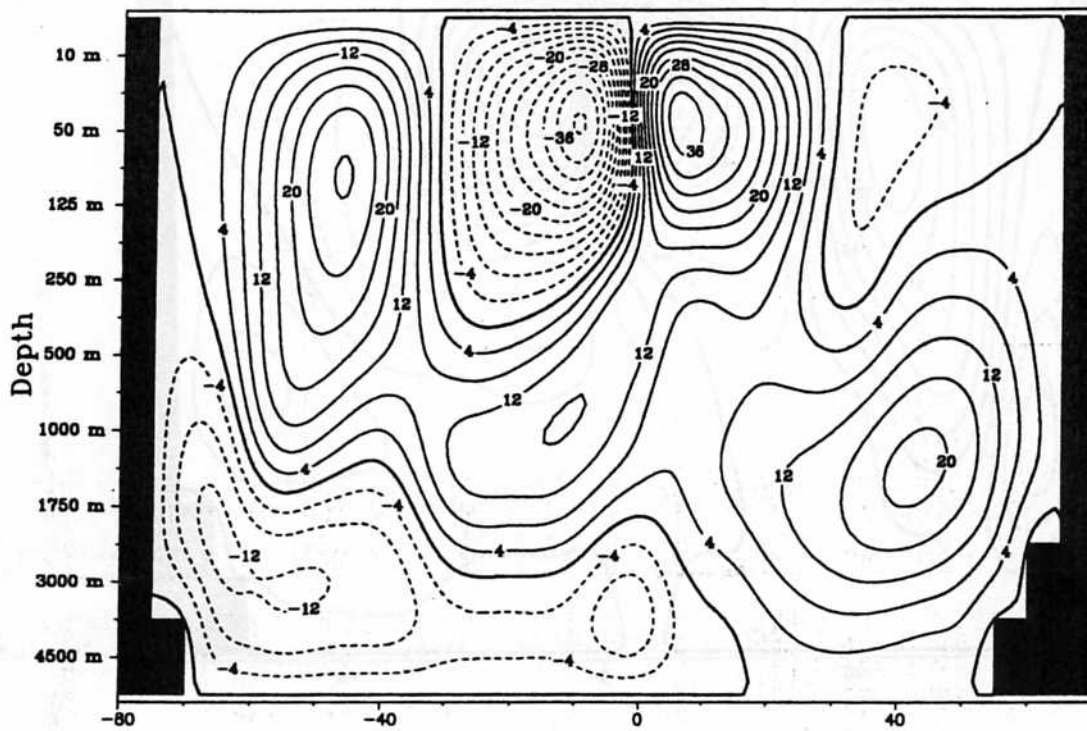


Figure 4.4. Global meridional streamfunction (in Sverdrups) obtained in the robust diagnostic experiment. The Southern Hemisphere is on the left hand side.

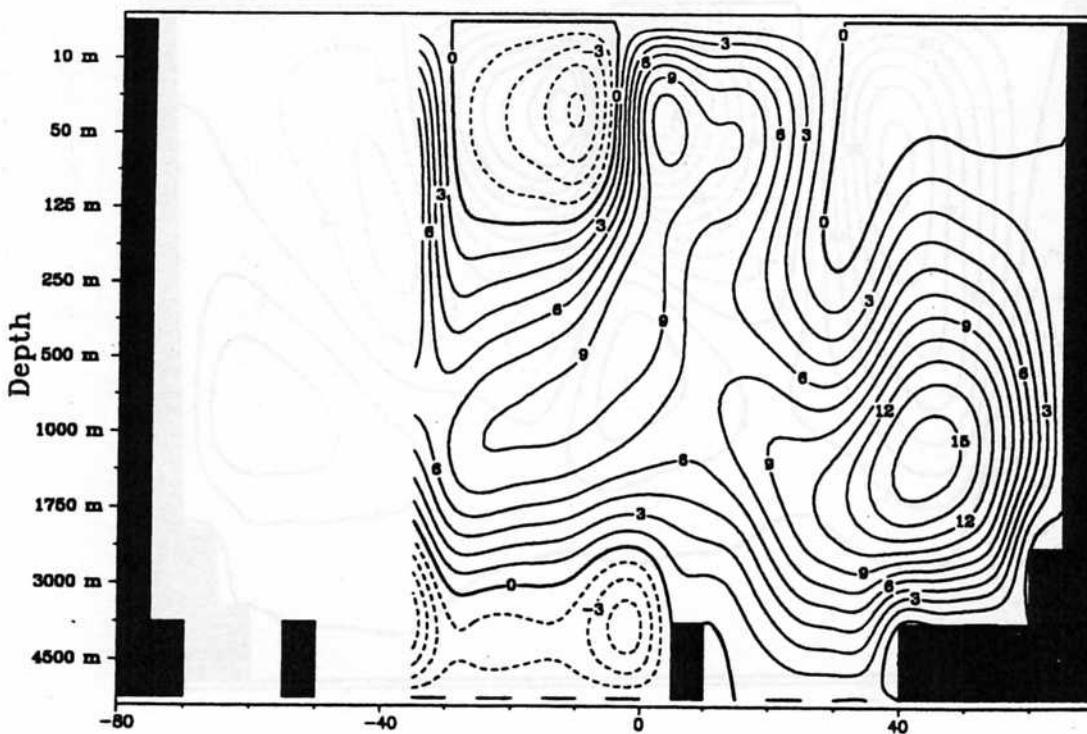


Figure 4.5. Atlantic overturning circulation (in Sverdrups) predicted in the robust diagnostic mode. The Southern Hemisphere is on the left hand side.



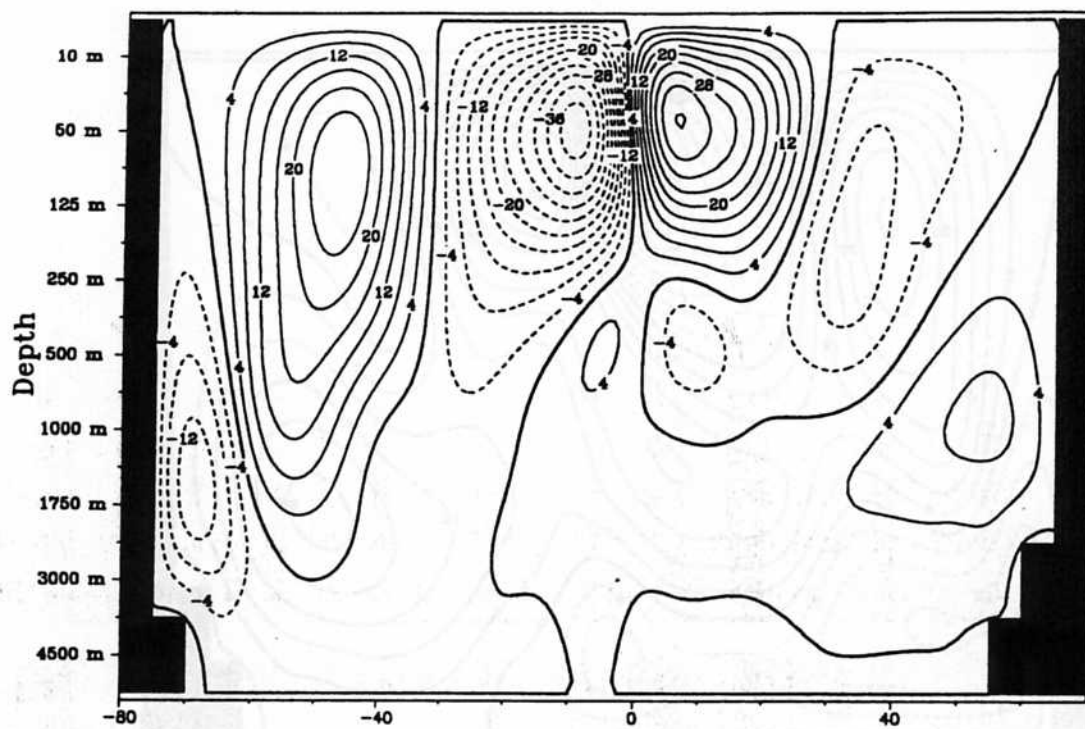


Figure 4.6. Global overturning streamfunction (in Sverdrups) from ASTR's model (steady state obtained without restoring terms). The Southern Hemisphere is on the left hand side.

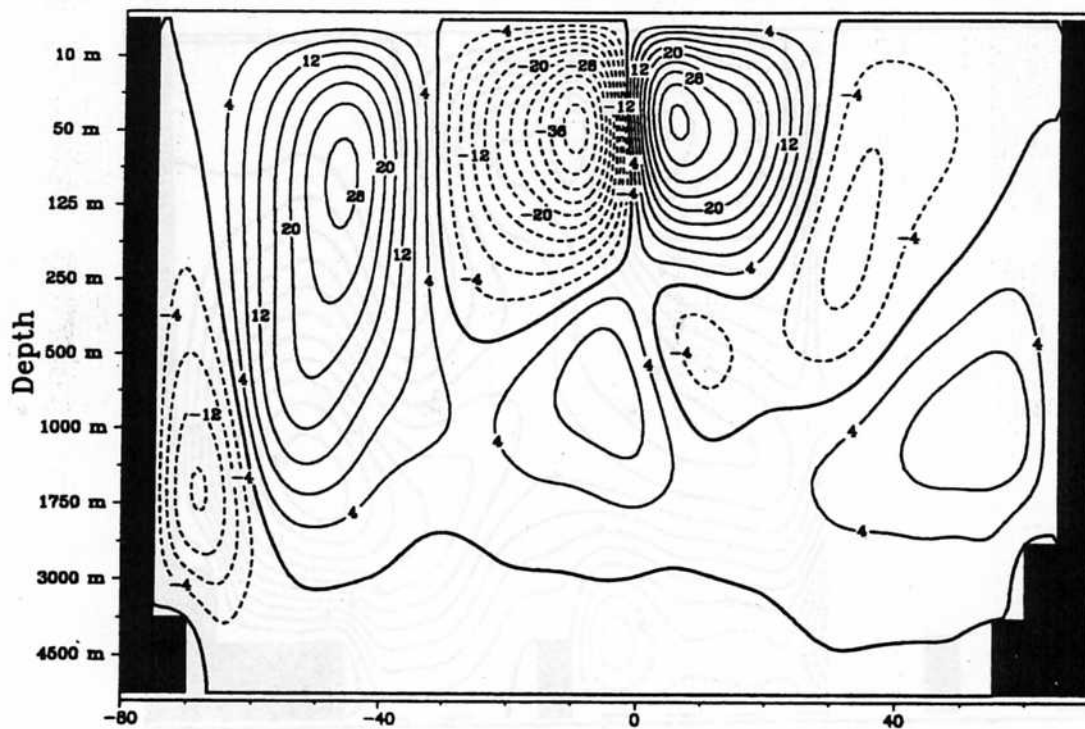


Figure 4.7. Global overturning streamfunction (in Sverdrups) obtained with the Semtner and Chervin model (steady state obtained without restoring terms). The Southern Hemisphere is on the left hand side.

### 4.3 Towards climatic simulations

It is clear that no truly climatic simulation can be carried out in robust diagnostic mode. Thus, whenever the robust diagnostic experiment are deemed satisfactory, the restoring terms must be removed. In this case, because the time scale of the deep ocean are very long, it takes thousands of years to reach a steady state.

The steady global overturning circulation (Figure 4.6) is not radically different from that obtained in robust diagnostic mode, which is very encouraging. Furthermore, the Semtner and Chervin model, when operated on the same grid and under the same forcings, leads to quite similar results (Figure 4.7). However, certain features are clearly too weak, such as the Northern Atlantic overturning circulation.

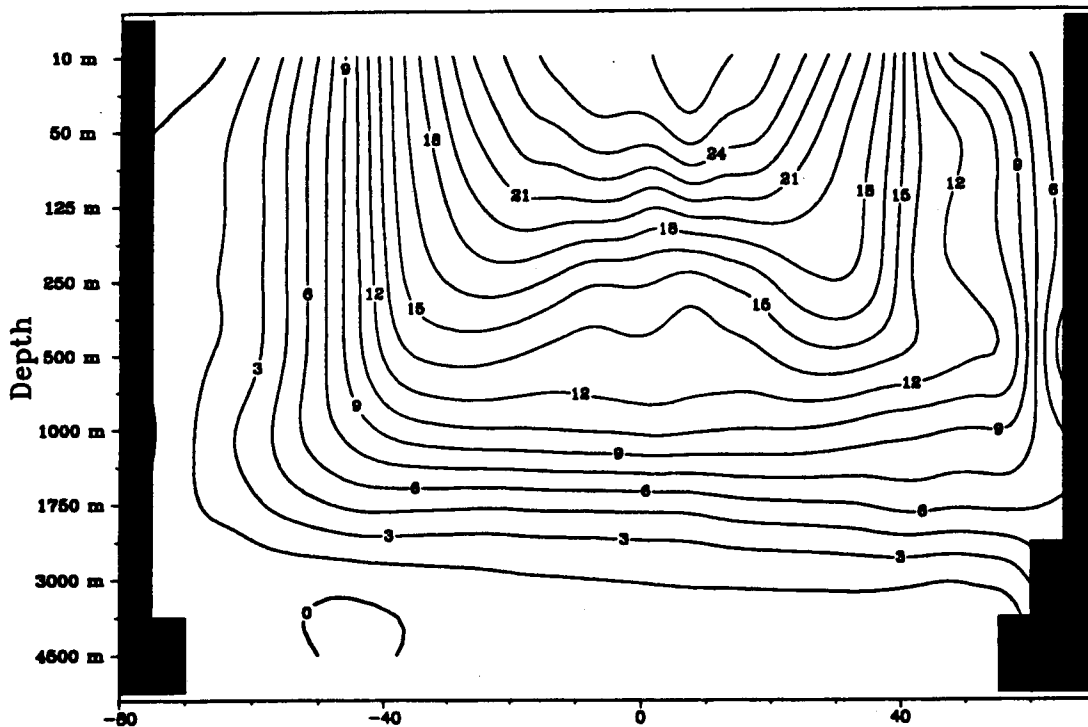


Figure 4.8. Zonally averaged temperature field from ASTR's model (steady state obtained without restoring terms). The Southern Hemisphere is on the left hand side.

The differences between the modelled temperature/salinity fields and the observations are illustrated in Table I. The zonally averaged temperature fields are depicted in Figure 4.8, which clearly shows that the intermediate water masses are a few degrees too warm. This might be due to the vertical resolution being significantly too coarse.

Table I. Measures of the temperature  $T$  and salinity  $S$  deviations with respect to the Levitus (1982) climatology ( $T_{Lev}$ ,  $S_{Lev}$ ) obtained in the “climatic steady state”, *i.e.*, without restoring terms in the equations governing the evolution of  $T$  and  $S$ . The operator “ $\langle \rangle$ ” denotes the average over the computational domain.

temperature deviation	salinity deviation
$\langle T - T_{Lev} \rangle = 1.4 \text{ }^\circ\text{K}$	$\langle S - S_{Lev} \rangle = 0.04 \text{ }^\circ\text{‰}$
$\langle  T - T_{Lev}  \rangle = 1.9 \text{ }^\circ\text{K}$	$\langle  S - S_{Lev}  \rangle = 0.22 \text{ }^\circ\text{‰}$

Here what is referred to as “steady state” is the solution of the equations obtained after approximately thousand years of integration from an initial state corresponding to a robust-diagnostic solution. After a few hundreds of years, the warming trend significantly decreases. A very careful analysis of the seemingly steady solution might however reveal the existence of a persistent global warming rate of order  $0.1 \text{ }^\circ\text{K}$  per millenium (Madec, 1993, personal communication). Coupling the OGCM with a sea ice model is probably the only way to avoid this problem — if it exists in our model — (Madec, 1993, personal communication). This will be examined.

## 5. CONCLUSION

It is obviously too soon to draw final conclusions about the research project presented here, mainly because the activities started only two years ago. Moreover, the OGCM and the sea ice model are still under development so that only preliminary results are presently available. No coupling of models has been attempted yet. However, the results presented in this report are very encouraging and point to the validity of our work. The AGCM of the LMD has been successfully implemented on our computers. The sea ice model, though coupled to a simple one-dimensional ocean model, is already giving realistic results. Finally, our free-surface OGCM provides good results in the robust diagnostic mode and the first simulation performed without restoring terms was deemed fairly satisfactory, despite the very coarse grid utilized and the non-global coverage of the World Ocean.

Future activities will include long term runs of LMD's AGCM and the implementation of the “dynamic part” of the sea ice model. The OGCM will continue to be used on the present grid for validation purposes, while the global version will be prepared. The first coupling to be tested will probably be between the global OGCM and the sea ice model. The coupling of the OGCM-sea ice model to the AGCM will be achieved at a later stage, probably during the second phase of the “Global Change” programme.



## ACKNOWLEDGEMENTS

The development of a model of the climate system is carried out within the scope of the Impulse Programme "Global Change" (Belgian State, Prime Minister's Services, Science Policy Office, Contract GC/10/013), the Convention d'Actions de Recherches Concertées No 092/97-154 with the Communauté Française de Belgique, the Impulse Programme "Information Technology" (Belgian State, Prime Minister's Services, Science Policy Office, Contract IT/SC/20), and a Study Contract between the Université Catholique de Louvain and IBM of Belgium s.a., which allows us to utilize an IBM RS/6000-550 workstation. Jean-Michel Campin has a research grant of the European Communities. Thierry Fichefet is supported by the National Fund for Scientific Research of Belgium. M. Morales Maqueda is funded by the Ministerio de Educacion y Ciencia of Spain under grant FPI-PG90. All these supports are gratefully acknowledged.

Many thanks are due to Robert Sadourny and, in general, to the Laboratoire de Météorologie Dynamique (CNRS, Paris) for providing us with the opportunity of installing LMD's AGCM on our computers. Hervé Grenier is particularly grateful to Hervé Le Treut, Claudio Menendez and Jan Polcher for their help in the development of a portable version of LMD's AGCM.

Thierry Fichefet thanks Serge Planton and, in general, the Centre National de Recherches Météorologiques (Météo-France, Toulouse) for processing the atmospheric data used to force the sea-ice model.

Eric Deleersnijder is indebted to Pascale Delecluse, Peter Killworth and Gurvan Madec for all their helpful comments about the development and the use of OGCMs.

## REFERENCES

- Beckers J.-M. 1991. Application of the GHER 3D general circulation model to the Western Mediterranean. *J. Mar. Syst.* 1: 315-332.
- Björk G. 1988. A one-dimensional time-dependent model for the vertical stratification of the upper Arctic Ocean. *J. Phys. Oceanogr.* 19: 52-67.
- Blumberg A.F. and Mellor G.L. 1987. A description of a three-dimensional coastal ocean circulation model. In: Three-dimensional coastal ocean models. Heaps N.S. (Ed). American Geophysical Union, Washington, D.C.:1-16.
- Bryan K. 1969. A numerical method for the study of the circulation of the World Ocean. *J. Comput. Phys.* 4: 347-376.
- Bryan K. 1984. Accelerating the convergence to equilibrium of ocean-climate models. *J. Phys. Oceanogr.* 14: 666-673.
- Carissimo B.C., Oort A.H. and Vonder Haar T.H. 1985. Estimating the meridional energy transports in the atmosphere and oceans. *J. Phys. Oceanogr.* 15: 82-91.
- Cess R.D., Potter G.L., Blanchet J.P., Boer G.J., Del genio A.D., Déqué M., Dymnikov V., Galin V., Gates W.L., Ghan S.J., Kiehl J.T., Lacis A.A., Le Treut H., Li Z.-X., Liang X.-Z., McAvaney B.J., Meleshko V.P., Mitchell J.F.B., Morcrette J.-J., Randall D.A., Rikus L., Roeckner E., Royer J.F., Schlese U., Sheinin D.A., Slingo A., Sokolov A.P., Taylor K.E., Washington W.M., Wetherald R.T., Yagai I. and Zhang M.-H. 1990. Intercomparison and interpretation of climate feedback processes in nineteen atmospheric general circulation models. *J. Geophys. Res.* 95: 16,601-16,615.
- Cubash U., Hasselmann K., Höck H., Maier-Reimer E., Mikolaewicz U., Santer B. and Sausen R. 1992. Time-dependent greenhouse warming computations with a coupled ocean-atmosphere model. *Clim. Dyn.* 8: 55-69.
- Deleersnijder and Campin J.-M. 1993a. A brief description of ASTR's free surface ocean general circulation model. Progress Report 1993/6. Institut d'Astronomie et de Géophysique G. Lemaître, Université Catholique de Louvain, Louvain-la-Neuve. (in preparation).

- Deleersnijder and Campin J.-M. 1993b. Du calcul de la position de la surface de l'océan dans un modèle de circulation générale. Contribution No 70. Institut d'Astronomie et de Géophysique G. Lemaître, Université Catholique de Louvain, Louvain-la-Neuve. 26 p.
- Deleersnijder E. and Luyten P. 1993. On the practical advantages of the quasi-equilibrium version of the Mellor and Yamada level 2.5 turbulence closure applied to marine modelling. Contribution No 69. Institut d'Astronomie et de Géophysique G. Lemaître, Université Catholique de Louvain, Louvain-la-Neuve. 15 p.
- Ducoudré N.I., Laval K. and Perrier-Sechiba A. 1993. A new set of parameterizations of the hydrological exchanges at the land/atmosphere interface within the LMD Atmospheric General Circulation Model. *J. Clim.* (in press).
- Fichefet T. and Gaspar P. 1988. A model study of upper ocean – sea ice interactions. *J. Phys. Oceanogr.* 18: 181–195.
- Fichefet T. and Maqueda M.M. 1993. An upper ocean – sea-ice model for climate studies. Progress Report 1993/4. Institut d'Astronomie et de Géophysique G. Lemaître, Université Catholique de Louvain, Louvain-la-Neuve. 17 p.
- Flato G.M. and Hibler III W.D. 1982. Modeling pack ice as a cavitating fluid. *J. Phys. Oceanogr.* 22: 626–651.
- Fouquart Y. and Bonnel B. 1980. Computation of solar heating of the Earth's atmosphere: a new parameterization. *Beitr. Phys. Atmos.* 53: 35–62.
- Gadd A.J. 1978. A split-explicit integration scheme for numerical weather prediction. *Q. J. R. Meteorol. Soc.* 104: 1093–1104.
- Gaspar P. 1988. Modeling the seasonal cycle of the upper ocean. *J. Phys. Oceanogr.* 18: 161–180.
- Grenier H. 1993. Le modèle de circulation générale atmosphérique du LMD: justification du choix de l'AGCM du LMD pour l'élaboration d'un modèle couplé océan-atmosphère. Progress Report 1993/3. Institut d'Astronomie et de Géophysique G. Lemaître, Université Catholique de Louvain, Louvain-la-Neuve. 16 p.
- Hellerman S. and Rosenstein M. 1983. Normal monthly wind stress over the world ocean with error estimates. *J. Phys. oceanogr.* 13: 1093–1104.
- Hibler III W.D. 1979. A dynamic thermodynamic sea ice model. *J. Phys. Oceanogr.* 9: 815–846.
- Hibler III W.D. 1980. Modeling a variable thickness sea ice cover. *Mon. Weather Rev.* 108: 1943–1973.
- Houghton J.T., Jenkins G.J. and Ephraums J.J. (Eds.). 1990. Intergovernmental panel on climate change – Climate change: the IPCC scientific assessment. Cambridge University Press, Cambridge. 364 p.
- Houghton J.T., Callander B.A. and Varney S.K. (Eds.). 1992. Intergovernmental panel on climate change – Climate change 1992: the supplementary report to the IPCC scientific assessment. Cambridge University Press, Cambridge. 200 p.
- James I.D. 1986. A front resolving sigma coordinate sea model with a simple hybrid advection scheme. *Appl. Math. Model.* 10: 87–92.
- Killworth P.D., Stainforth D., Webb D. and Paterson S.M. 1991. The development of a free-surface Bryan-Cox-Semtner ocean model. *J. Phys. Oceanogr.* 21: 1333–1348.
- Le Treut H. and Li Z.X. 1991. Sensitivity of an atmospheric general circulation model to prescribed SST changes: feedback effects associated with the simulation of cloud optical properties. *Clim. Dyn.* 5: 175–187.
- Levitus S. 1982. Climatological atlas of the world oceans. NOAA Prof. Paper 13, U.S. Gov. Print. Office, Washington, D.C., 173 p.
- Madala R.V. 1981. Efficient time integration schemes for atmosphere and ocean models. In: Finite-difference techniques for vectorized fluid dynamics calculations. Book D.L. (Ed). Springer-Verlag: 56–74.
- Maier-Reimer E., Mikolajewicz U. and Hasselmann K. 1991. On the sensitivity of the global ocean circulation to changes in the surface heat flux forcings. Rep. No. 68. Max-Planck-Institut für Meteorologie, Hamburg. 67 p.

- Maqueda M.M. and Fichefet T. 1991. ECT: an eddy kinetic energy model of the oceanic vertical mixing. Progress Report 1991/1. Institut d'Astronomie et de Géophysique G. Lemaître, Université Catholique de Louvain, Louvain-la-Neuve. 83 p.
- Marti O. 1992. Etude de l'Océan Mondial: modélisation de la circulation et du transport des traceurs anthropiques. Thèse de Doctorat. Université de Paris VI, Paris. 201 p.
- McPhee M. 1975. Ice ocean momentum transfer for the AIDJEX model. AIDJEX Bull. 29: 93-111.
- Mesinger F. and Arakawa A. 1976. Numerical methods used in atmospheric models (Volume 1). GARP Publications Series No. 17, WMO-ICSU, 64 p.
- Morcrette J.J. 1991. Radiation and cloud radiative properties in the European Centre for Medium Range Weather Forecasts forecasting systems. J. Geophys. Res. 96: 9121-9132.
- Pacanowski R.C. and Philander S.G.H. 1981. Parameterization of vertical mixing in numerical models of tropical oceans. J. Phys. Oceanogr. 11: 1443-1451.
- Parkinson C.L., Comiso J.C., Zwally H.J., Cavalieri D.J., Gloersen P. and Campbell W.J. 1987. Arctic sea ice, 1973-1976: satellite passive microwave observations. NASA, Washington, D.C., 296 p.
- Peixoto J.P. and Oort A.H. 1992. Physics of climate. American Institute of Physics, New York. 520 p.
- Phillips N.A. 1957. A coordinate system having some special advantages for numerical forecasting. J. Meteorol. 14: 184-185.
- Polcher J. and Laval K. 1993. The impact of African and Amazonian deforestation on tropical climate. J. Hydrol. (submitted).
- Prather M.J. 1986. Numerical advection by conservation of second order moments. J. Geophys. Res. 91: 6671-6681.
- Rothrock D.A. 1973. Circulation of an incompressible ice cover. AIDJEX Bull. 18: 61-68.
- Semtner A.J. 1974. An oceanic general circulation model with bottom topography. Numerical simulation of weather and climate, Tech. Rep. No. 9. Dept. of Meteorol. UCLA, 99 p.
- Semtner A.J. 1976. A model for the thermodynamic growth of sea ice in numerical investigations of climate. J. Phys. Oceanogr. 6: 379-389.
- Semtner A.J. 1986. Finite-difference formulation of a World Ocean model. In: Advanced physical oceanographic numerical modelling. O'Brien J.J. (Ed). Reidel, Dordrecht: 187-202.
- Semtner A.J. 1987. A numerical study of sea ice and ocean circulation in the Arctic. J. Phys. Oceanogr. 17: 1077-1099.
- Semtner A.J. and Chervin R.M. 1988. A simulation of the global ocean circulation with resolved eddies. J. Geophys. Res. 93: 15502-15522, 15767-15775.
- Semtner A. and Chervin R.M. 1992. Ocean general circulation from a global eddy-resolving model. J. Geophys. Res. 97: 5493-5550.
- Thorndike A.S. 1986. Kinematics of sea ice. In: Geophysics of Sea Ice. Untersteiner N. (Ed.). NATO ASI series, Vol. 146, Plenum Press, New York: 489-549.
- Toggweiler J.R., Dixon K. and Bryan K. 1989. Simulation of radiocarbon in a coarse-resolution World Ocean model. 1. Steady state prebomb distributions. J. Geophys. Res. 94: 8217-8242.
- Van den Eynde D. 1992. Literature study of the inclusion of a turbulence model in the global oceanic circulation model of Semtner and Chervin. Rep. MUMM/GC/TR01. 10 p.
- van Ypersele J.-P. 1986. A numerical study of the response of the Southern Ocean and its sea ice to a CO<sub>2</sub>-induced atmospheric warming. Cooperative thesis No 99. NCAR/CT-99, National Center for Atmospheric Research and Université Catholique de Louvain, Boulder and Louvain-la-Neuve. 135+XV p.
- van Ypersele J.-P. 1990. Modelling sea ice for climate studies. In: Climate-Ocean Interaction. Schlesinger M.E. (Ed). Kluwer Academic Publishers, Dordrecht: 97-123.
- Zwally H.J., Comiso J.C., Parkinson C.L., Campbell W.J., Carsey F.D. and Gloersen P. 1983. Antarctic sea ice, 1973-1976: satellite passive microwave observations. NASA, Washington, D.C., 206 p.